International Journal of Electronics and Communication Engineering.
ISSN 0974-2166 Volume 4, Number 3 (2011), pp. 287-293

http://www.irphouse.com

Mutual Coupling between Two Patches using Ideal High Impedance Surface

Vikas Kaduskar and R.S. Kawitkar

Dept. of Electronics, BVDUCOE, Pune, India
Dept. of E & TC, SCOE, Pune, India

Abstract

A design of a High Impedance Surface (HIS) is proposed. According to the simulated performances of this HIS, an ideal HIS is defined as a Perfect Magnetic Conductor (PMC). Based on this approximation, a study about the positioning of the HIS between two microstrip antennas is carried out.

Keywords: High Impedance surface, Mutual conductance, Microstrip Patch.

Introduction
In this paper, an investigation of the means of minimizing the mutual coupling will be carried out. In the first part, the design of a HIS will be presented, together with a new approach of modellisation. In the second part, an investigation of the mutual coupling reduction will be carried out by varying the position of the ideal HIS between two adjacent patches.

Coupling between Patches
The coupling between two or more microstrip antenna elements can be taken into account easily using full-wave analyses. However, it is more difficult to do using the transmission-line and cavity models, although successful attempts have been made using the transmission-line model [75] and the cavity model . It can be shown that coupling between two patches, as is coupling between two aperture or two wire antennas, is a function of the position of one element relative to the other. For two rectangular microstrip patches the coupling for two side-by-side elements is a function of the relative alignment. When the elements are positioned collinearly along the *E*-plane, this arrangement is referred to as the *E-plane*, as shown in Figure 1 (a); when the elements are positioned collinearly along the *H*-plane, this arrangement isreferred to as the *H-plane*, as shown in Figure 1 (b). For an edge-to-edge separation

of *s*, the *E*-plane exhibits the smallest coupling isolation for very small spacing (typically $s < 0.10\lambda 0$) while the *H*-plane exhibits the smallest coupling for large spacing (typically $s > 0.10\lambda 0$). The spacing at which one plane coupling overtakes the other one depends on the electrical properties and geometrical dimensions of the microstrip antenna. Typical variations are shown in Figure 2.

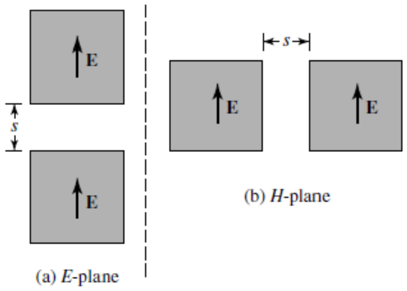

Figure 1: *E*- and *H*-plane arrangements of microstrip patch antennas.

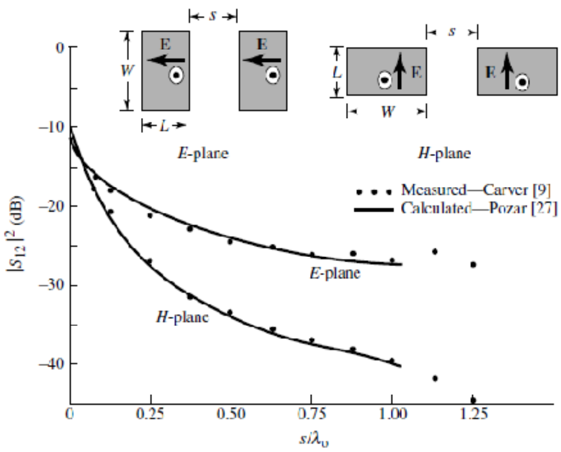

Figure 2: Measured and calculated mutual coupling between two coax-fed microstrip antennas, for both *E*-plane and *H*-plane coupling, (W = 10.57 cm, L = 6.55 cm, h = 0.1588 cm, εr = 2.55, fr = 1,410 MHz).

In general, mutual coupling is primarily attributed to the fields that exist along the air-dielectric interface. The fields can be decomposed to space waves (with $1/\rho$ radial variations), higher order waves (with $1/\rho 2$ radial variations), surface waves (with $1/\rho 1/2$ radial variations), and leaky waves [with $\exp(-\lambda\rho)/\rho 1/2$ radial variations]. Because of the spherical radial variation, space $(1/\rho)$ and higher order waves $(1/\rho 2)$ are most dominant for very small spacing while surface waves, because of their $1/\rho 1/2$ radial variations are dominant for large separations. Surface waves exist and propagate within the dielectric, and their excitationis a functionof the thickness of the substrate [79]. In a given direction, the lowest order (dominant) surface wave mode is

TM(odd) with zero cutoff frequency followed by a TE(even), and alternatively by TM(odd) and TE(even) modes. For a rectangular microstrip patch, the fields are TM in a direction of propagation along the *E*-plane and TE in a direction of propagation along the *H*-plane. Since for the *E*-plane arrangement of Figure 1 (a) the elements are placed collinearly along the *E*-plane where the fields in the space between the elements are primarily TM, there is a stronger surface wave excitation (based on a single dominant surface wave mode) between the elements, and the coupling is larger. However for the *H*-plane arrangement of Figure 1(b), the fields in the space between the elements are primarily TE and there is not a strong dominant mode surface wave excitation; therefore there is less coupling between the elements. This does change as the thickness of the substrate increases which allows higher order TE surface wave excitation. The mutual conductance between two rectangular microstrip patches has also been found using the basic definition of conductance given by (1),

$$G_{12} = \frac{1}{|V_0|^2} \mathrm{Re} \iint_S \mathbf{E}_1 \times \mathbf{H}_2^* \cdot d\mathbf{s} \tag{1}$$

the far fields based onthe cavity model, For the *E*-plane arrangement of Figure 1 (a) and for the odd mode field distribution beneath the patch, which is representative of the dominant mode, the mutual conductance is

$$G_{12} = \frac{1}{\pi}\sqrt{\frac{\epsilon}{\mu}} \int_0^{\pi} \left[\frac{\sin\left(\frac{k_0 W}{2}\cos\theta\right)}{\cos\theta} \right]^2 \sin^3\theta \left\{ 2J_0\left(\frac{Y}{\lambda_0}2\pi\sin\theta\right) + J_0\left(\frac{Y+L}{\lambda_0}2\pi\sin\theta\right) + J_0\left(\frac{Y-L}{\lambda_0}2\pi\sin\theta\right) \right\} d\theta \tag{2}$$

where Y is the center-to-center separation between the slots and $J0$ is the Bessel function of the first kind of order zero. The first term in (2) represents the mutual conductance of two slots separated by a distance X along the *E*-plane while the second and third terms represent, respectively, the conductance's of two slots separated along the *E*-plane by distances $Y + L$ and $Y - L$. Typical normalized results are shown by the solid curve in Figure 3. For the *H*-plane arrangement of Figure 1 (b) and for the odd mode field distribution beneath the patch, which is representative of the dominant mode, the mutual conductance is

$$G_{12} = \frac{2}{\pi}\sqrt{\frac{\epsilon}{\mu}} \int_0^{\pi} \left[\frac{\sin\left(\frac{k_0 W}{2}\cos\theta\right)}{\cos\theta} \right]^2 \sin^3\theta \cos\left(\frac{Z}{\lambda_0}2\pi\cos\theta\right) \cdot \left\{ 1 + J_0\left(\frac{L}{\lambda_0}2\pi\sin\theta\right) \right\} d\theta \tag{3}$$

where Z is the center-to-center separation between the slots and $J0$ is the Bessel function of the first kind of order zero. The first term in (3) represents twice the mutual conductance of two slots separated along the *H*-plane by a distance Z while the second term represents twice the conductance between two slots separated along the

E-plane by a distance *L* and along the *H*-plane by a distance *Z*. Typical normalized results are shownby the dashed curve inFigure 14.31. By comparing the results of Figure 14.31 it is clear that the mutual conductance for the *H*-plane arrangement, as expected, decreases with distance faster than that of the *E*-plane. Also it is observed that the mutual conductance for the *E*-plane arrangement is higher for wider elements while it is lower for wider elements for the *H*-plane arrangement.

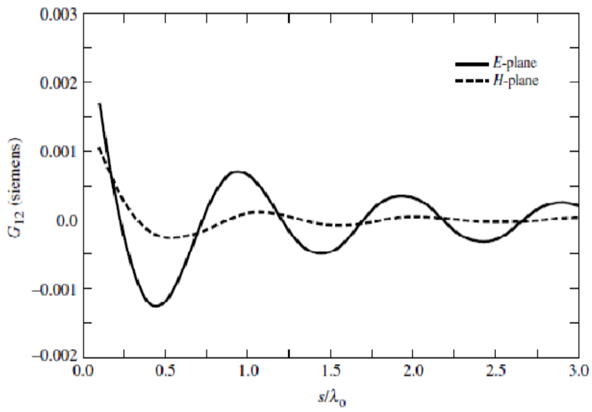

Figure 3: *E*- an d*H*-plane mutual conductance versus patch separation for rectangular microstrip patch antennas *(W* = 1.186 cm*, L* = 0.906 cm*, Ir* = 2.2*, λ*0 = 3 cm*).*

High Impedance Surfaces

By incorporating a special texture on a conductor, it is possible to alter its radiofrequency surface properties. In the limit where the period of the surface texture is much smaller than the wavelength, the structure can be described using an effective medium model, and its qualities can be summarized into a single parameter, the surface impedance. This boundary condition defines the ratio of the tangential electric field to the tangential magnetic field at the surface. It is the same impedance given by Ohm’s law: the ratio of the voltage to the current along the sheet, expressed in Ohms/square. A smooth conducting sheet has low surface impedance, while with a specially designed geometry, the textured surface can have high surface impedance.

Figure 4: Cross-section of a high-impedance surface.

A high-impedance surface, shown in cross section in Figure 4, consists of an array of metal protrusions on a flat metal sheet. They are arranged in a two-dimensional lattice, and are usually formed as metal plates, connected to the continuous lower conductor by vertical posts. They can be visualized as mushrooms or thumbtacks protruding from the surface. An example of a top view is shown in Figure 5.

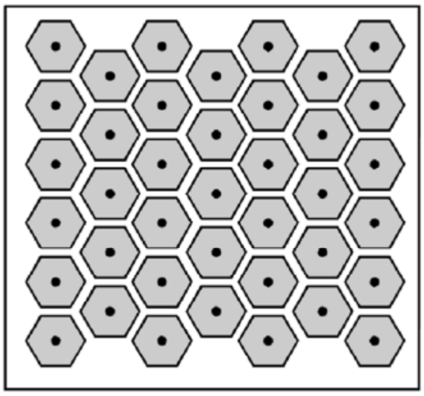

Figure 5: Top view of the high-impedance surface.

The hexagonal metal patches are raised above the surface, and the dots in the center are vertical connecting posts. If the protrusions are small compared to the wavelength, their electromagnetic properties can be described using lumped circuit elements – capacitors and inductors. The proximity of the neighboring metal elements provides the capacitance, and the long conducting path linking them together provides the inductance. They behave as parallel resonant LC circuits, which act as electric filters to block the flow of currents along the sheet. An equivalent circuit is shown below in Figure 6. This is the origin of the high electromagnetic surface impedance.

Figure 6: An equivalent circuit for the high-impedance surface.

The benefits arise from the reflection phase, which allows for low-profile antennas, and from the suppression of surface current propagation, which has been shown to produce improvements in the radiation pattern. A quantitative analysis of the degree of coupling between nearby antennas has a bearing on the design of large, multi-element arrays, as well as the minimum size ground plane that can be used for a single, compact radiator. The coupling strength was determined by measuring the transmission between two antennas positioned near the high-impedance surface, and near a metal surface for comparison. For TM polarization, shown in Figure 7, the probe antennas were of the flared, parallel-plate waveguide type. They were moved across the surface, and the transmission between them was measured as a function of separation distance. For TE polarization, shown in Figure 8, wire antennas were aligned parallel to the surface. The data were taken at about 15 GHz, within the band gap of the high-impedance surface.

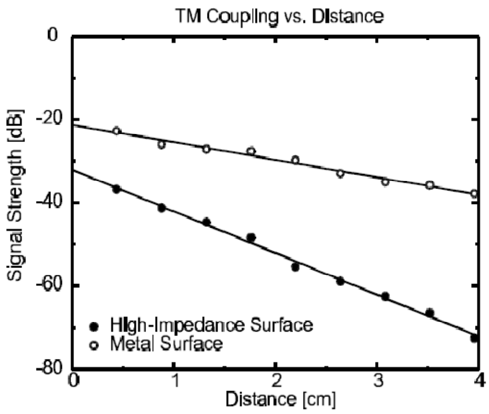

Figure 7: Coupling between two antennas in TM configuration.

Microwave absorbing foam was positioned several millimeters above the surface, in order to confine the measurement to the region just above the ground plane, and to eliminate interference from waves propagating through the surrounding space. The results represent a combination of two factors: the coupling strength from the antennas to the surface determines the intersection with the vertical axis, while the transmission across the surface is shown by the slope of each line. For TM polarization, shown in Figure 7, the coupling strength on the high-impedance surface is significantly reduced, and the signal decreases much more rapidly with distance than on the metal surface. However, for TE polarization, shown in Figure 8, the coupling strength on the high-impedance surface is greater than on the metal surface, and the signal decreases more slowly with distance.

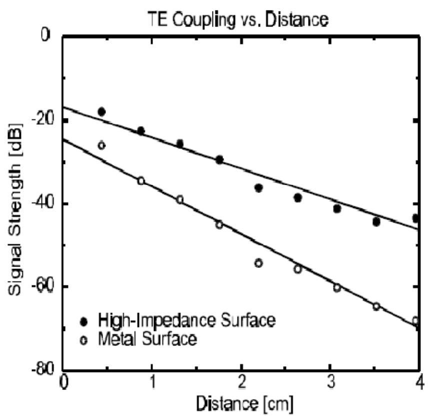

Figure 8: Coupling between two antennas in TE configuration.

This can be understood by interpreting the graphs from the viewpoint of the surface as a boundary condition. When an antenna is placed next to a flat metal surface, it generates plane waves, as well as currents in the surface. TM polarized waves and currents will readily be excited on a metal sheet, as the electric field is primarily perpendicular to the conductor The ensemble of fields and currents propagates unhindered by the metal, and radiates rather poorly. On the high-impedance surface, the situation is reversed. This can be understood by recalling that the high-impedance surface functions as a kind of magnetic conductor. Just as a metal surface repels transverse electric fields, the high-impedance surface abhors transverse magnetic fields. Hence, TM transmission is very small, as is the coupling strength to a TM polarized antenna. In other words, if a surface current with TM polarization is generated on the high-impedance surface, it will rapidly radiate.

Conclusions

It has been shown that such an approximation provides the possibility of simulating the effect of a HIS between the patches with limited amount of computing power. High Impedance surfaces, well known to suppress surface waves, demonstrate properties at its resonant frequency similar to perfect magnetic conductor. By inserting such structures between two patch antennas, it is thus possible to reduce the mutual coupling levels.

References

[1] H.L. Van Trees, ≪ Optimum Array Processing, Part IV of Detection, Estimation, and Modulation Theory ≫, WILEY-INTERSCIENCE 2002

[2] Ngai, E.C.; Blejer, D.J., "Mutual coupling analyses for small GPS adaptive arrays," Antennas and Propagation Society International Symposium, 2001. IEEE , vol.4, no., pp.38-41 vol.4, 2001.

[3] Jedlicka, R.; Poe, M.; Carver, K., "Measured mutual coupling between microstrip antennas," Antennas and Propagation, IEEE Transactions on , vol.29, no.1, pp. 147-149, Jan 1981

[4] Sievenpiper, D.; Lijun Zhang; Broas, R.F.J.; Alexopolous, N.G.; Yablonovitch, E., "High-impedance electromagnetic surfaces with a forbidden frequency band," Microwave Theory and Techniques, IEEE Transactions on , vol.47, no.11, pp.2059-2074, Nov 1999

[5] C.Balanis, Antenna Theory, Analysis, and Design, 2nd ed. New York: Wiley, 1997

[6] Fan Yang; Rahmat-Samii, Y., "Microstrip antennas integrated with electromagnetic band-gap (EBG) structures: a low mutual coupling design for array applications," Antennas and Propagation, IEEE Transactions on , vol.51, no.10, pp. 2936-2946, Oct. 2003